

MECHANISM FOR FINGER PERSISTENCE IN HOMOGENEOUS, UNSATURATED, POROUS MEDIA: THEORY AND VERIFICATION

ROBERT J. GLASS,¹ TAMMO S. STEENHUIS,² AND J.-YVES PARLANGE²

Wetting-front instability, or gravity-driven fingering, can occur during vertical infiltration. Previous studies found that fingers persist over long periods of constant infiltration and in subsequent infiltration cycles. We present a physically based theory to explain finger persistence. The theory is tested using a new technique in which moisture contents are visualized by the transmission of light through unsaturated sand, recorded with a video camera, and then analyzed by video digitizing computer hardware. Theory and experiments show that hysteresis in the moisture characteristic relationship explains the persistence of fingers in time.

The stability of the interface between two fluids in a porous medium has been the topic of continuous research in the fields of chemical engineering, fluid mechanics, and petroleum engineering since the discovery of interfacial instability by Hill (1952). The simple heuristic analysis of Hill and the first linear stability analysis of the problem presented by Saffman and Taylor (1958) recognize three factors influential in determining the stability of a steady, constant-velocity, one-dimensional, vertical downward displacement of one fluid (subscript 2) by another (subscript 1) in a homogeneous, isotropic porous medium: the fluid viscosity difference ($\mu_1 - \mu_2$); the fluid density difference ($\rho_1 - \rho_2$); and the interfacial velocity (U). Their result suggests that such a steady, planar displacement is unstable for all wavelengths when the inequality

$$kg(\rho_1 - \rho_2) - \theta_a U(\mu_1 - \mu_2) > 0 \quad (1)$$

is satisfied (k is the permeability of the media, θ_a is the pore volume available for fluid transport, and g is the gravitational acceleration). Though several assumptions have been made to

derive this criterion (e.g., the fluids are incompressible, Darcy's law holds for each fluid in the porous media, disturbances are infinitesimal, the mixing between the two fluids at the interface is negligible, and θ_a is the same for each fluid), the relationship between buoyant and viscous forces given in Eq. (1) is instructive. Flows are seen to be either stabilized or destabilized by viscosity and density differences, with the interfacial velocity multiplying the viscosity difference. The role of capillarity at the interface has not been included in the derivation of Eq. (1); however, when it is included, either through the heuristic approach of Chouke et al. (1959) or the more rigorous approach of Parlange and Hill (1976), it is found to limit the unstable wavelengths to be above a minimum value determined by the properties of the porous medium.

Most research in petroleum engineering has concentrated on viscosity-driven instabilities in the absence of gravity, termed *viscous fingering*; the reader is referred to a recent review of this rich literature by Homsy (1987). Gravity-driven instabilities in porous media have application to hydrology and soil physics where gravity plays a major role in the movement of water, air, and other fluids, both immiscible and miscible, through the subsurface. In the ubiquitous case of vertical infiltration, a liquid, usually water, moves downward into a porous medium filled with air and water. If we assume the velocity of the air and water interface to be constant (U), the interface to be sharp, and the air to undergo little compression, then we may apply Eq. (1) directly. We see in this case that the density difference is destabilizing, and that of viscosity is stabilizing. Because both the viscosity and the density of water are much greater than that of air, Eq. (1) simplifies to

$$\theta_a U < \frac{kg\rho_1}{\mu_1} = K_s \quad (2)$$

where K_s is the saturated hydraulic conductivity of the medium. Because $U\theta_a$ is simply the flux through the system, within the constraints of its

¹ Geoscience Analysis Div. 6315, Sandia National Laboratories, Albuquerque, N.M.

² Dept. of Agricultural and Biological Engineering, Cornell Univ., Ithaca, N.Y.

Received 29 Aug. 1988; revised 14 March 1989.

derivation, Eq. (2) predicts that all infiltration flows where water is supplied at a rate less than the saturated conductivity are unstable. Such potentially unstable situations often occur both in the field and in standard laboratory experiments. For example, the case of ponded infiltration into a two-layer system where the top layer is of lower conductivity than the bottom layer satisfies Eq. (2) as does the analogous laboratory experiment where a pressure plate is used to supply water to the top of a uniform soil column.

Although gravity-driven instabilities, or fingers, were noted in a number of experimental studies in soil physics (e.g., Tabuchi 1961; Miller and Gardener 1962; Peck 1965; and Smith 1967), Hill and Parlange (1972) first recognized the application of the inequality, Eq. (2), and conducted a series of experiments to demonstrate the instability of the macroscopic water and air interface when Eq. (2) is satisfied. They termed the instability "wetting-front instability," and the phenomenon has been the subject of a series of research efforts since (e.g., Raats 1973; Philip 1975*a,b*; Parlange and Hill 1976; White et al. 1976, 1977; Starr et al. 1978, 1986; Diment et al. 1982; Diment and Watson 1983, 1985; Glass and Steenhuis 1984; Glass et al. 1987, 1988, 1989*a,b*; Tamai et al. 1987; and Hillel and Baker 1988).

Beyond the testing of the simple theory resulting in the stability criterion, Eq. (2), a number of interesting facts concerning finger development and unstable flow-field behavior have been uncovered through experimentation. The development of fingers and the steady-state flow field that forms upon long-term ponded infiltration in an initially uniformly dry, fine-over-coarse-textured, layered sand system was shown qualitatively through the use of dyes and photographic documentation by Glass and Steenhuis (1984) and Glass et al. (1987). The flat, downward-moving wetting front in the top fine layer becomes unstable as it passes into the bottom coarse layer, causing the formation of fingers in the coarse layer. Three stages in the evolution of the unstable flow field were noted. The initial stage is dominated by rapid downward movement of fingers that form finger "core" areas. When supplied at a constant flow rate, fully developed fingers maintain a constant finger tip velocity and widen rapidly to a constant width as the finger tip passes. Glass et al. (1989*a,b*) have quantified relationships in this stage among flow through the finger, finger

width, and finger velocity. In general, the higher the flow, the wider the finger and the higher the velocity of the finger tip. The second stage is characterized by the persistence of finger core areas that continue to conduct most of the flow and by the slow lateral movement of wetting fronts with less moisture from finger core areas into the surrounding dry sand. A less saturated "fringe" area thus develops between the more saturated finger core areas. The lateral movement in the second stage is slow, having a time scale on the order of days, but the time scale for the downward finger growth in the first stage is much faster, on the order of minutes. The final stage is a steady-state flow field in which core and fringe areas coexist for long periods of steady infiltration. Both the second and last phases, which had not been noted by earlier experimental studies (Hill and Parlange 1972; Diment and Watson 1985), demonstrate the important feature of core/fringe structure formation.

In addition to demonstrating the formation of the core/fringe structure during steady infiltration events, Glass and Steenhuis (1984) and Glass et al. (1987) also demonstrated the persistence of fingers from one infiltration cycle to the next. After an interruption in the water supply and drainage to field capacity, fingers form in the same locations as they did in the first cycle and have the same core areas, which continue to conduct almost all of the water. Fringe-area contribution is higher than in the first cycle, and a steady-state flow field is achieved much more rapidly. If the chamber is flooded and drained so that the initial moisture content field is made uniform, core areas are obliterated, thus emphasizing that finger persistence was not caused by heterogeneities in the porous material either in the initial pack or because of possible reorientation of grains by the initial fingers themselves.

In this paper, we present a physically based theory to explain the mechanism of finger persistence, and we verify the theory through experimentation. We develop an experimental technique to rapidly visualize the moisture content field in thin slabs of porous media. The technique is applied to carefully document the moisture content structure of fingers as they move downward and the persistence of finger structures in a second infiltration event after an interruption in water supply.

THEORY

A clue to understanding finger persistence was uncovered in an early study by Raats (1973), who discussed Tabuchi's (1961) finding that the potential of the water at a finger tip is less negative than that at the sides of the finger after the finger tip has passed. Raats stated: "It appears to me that this may be due to the fact that the capillary pressure head at the tip of the (fingers) corresponds to the point on the water content-capillary pressure head curve for wetting, while that at the stationary or receding part corresponds to the one for drying." In agreement with Raats' interpretation, we have observed that some individual pores empty a short distance behind the finger tip, thus decreasing the moisture content. When drying behind the finger tip occurs, the three stages in the development of the unstable flow field and finger persistence over repeated infiltration cycles can be explained quite simply.

Figure 1 is a sketch of a finger moving within an initially uniformly dry porous medium. Three zones within the vertically extending finger core area are shown. At the tip is a zone of high moisture content, θ_i , very near or at the satura-

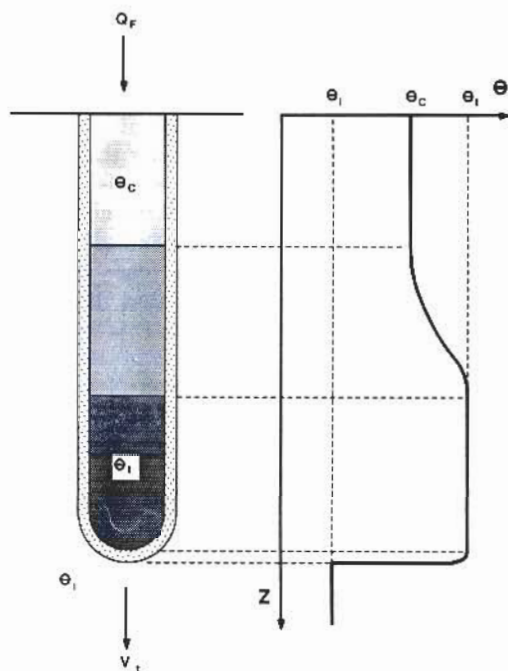


FIG. 1. A conceptual finger moving downward through porous media.

ted value, θ_i , followed by a zone of drying where the finger core passes from θ_i to θ_c , the moisture content of the finger core. Fingers have a constant tip velocity v_f , and θ_c is directly related to v_f . Surrounding the entire core area on all sides is a narrow zone of wetting where the moisture content increases rapidly from θ_i in the dry porous medium to the moisture content in the finger core.

Drying behind the tip decreases the matric potential and essentially halts rapid finger-core widening because of the sensitivity of the sorptivity to the potential at which the water is supplied. A uniform finger-core width only a short distance behind the finger tip is thus created. The two characteristics of the second phase of unstable flow-field development, i.e., the slow lateral widening of the fringe, compared with the rapid downward movement in the cores, and the lower moisture content in the fringe area, are direct consequences of the drying process behind the finger tip. The lateral movement of water from the finger core into the dry sand on either side of the finger takes place from a supply potential in the core that is less than what occurred when the finger tip passed. For an indefinitely long period of steady flow, lateral movement continues until the potential everywhere in the horizontal direction is the same. Because the sand in the fringe areas is becoming wet and that in the finger core areas is drying, then, as a result of hysteresis, two distinct moisture content zones coexist when the potential is equilibrated in the horizontal, thus yielding the observed third stage in unstable flow-field development.

With the use of a moisture characteristic relation that includes hysteresis, the theory may be explained in more detail. Figure 2 is a plot of matric potential, ψ , versus the moisture content, θ , for a typical sand. Considering a point on the axis of a finger, as the wet finger tip moves into dry porous medium, the wetting curve is descended to the point (θ_i, ψ_i) very near or at (θ_s, ψ_{sat}) , the saturated value of the moisture content and water entry value of the matric potential, respectively. After the tip passes, the matric potential decreases to the value ψ_{ar} , at which point the finger core begins to dry. A drying curve is thus ascended from the point (θ_i, ψ_i) to the point (θ_c, ψ_c) , where the moisture content of the finger core, θ_c , is less than θ_i and the corresponding matric potential ψ_c is less than the air

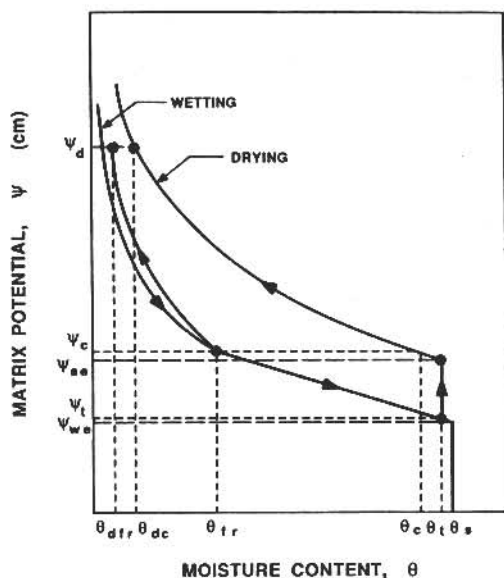


FIG. 2. Moisture characteristic curve with hysteresis for a typical sand showing development of core and fringe areas. Dots designate points on the curves discussed in the text. Note that ψ increases upward on the plot.

entry value ψ_{ac} . On a longer time scale, the dry sand on either side of the finger now wets by coming down the wetting curve until it reaches the matric potential ψ_c . Figure 2 shows that the moisture content in the finger core, θ_c , and that in the fringe area, θ_f , can be substantially different. This difference is observed in the final stage of the unstable flow-field development for infiltration into initially dry porous media. Thus, at equilibrium, two zones of different moisture content can coexist, and, because of the strong variation of the hydraulic conductivity with moisture content, almost all of the flow continues to take place through the finger cores as observed (with flux equal to the hydraulic conductivity, $K(\theta_c)$, in the core area).

When infiltration stops at the end of the first infiltration cycle, the moisture drains out of the finger core area, and the main drying curve is ascended to the point (θ_{dc}, ψ_d) when the water essentially stops flowing. ψ_d varies in the vertical and offsets the change in the gravity potential with depth when flow stops. The fringe areas also drain, and the matric potential moves to the value ψ_d ; however, it follows the scanning curve shown in Fig. 2 to the point (θ_{df}, ψ_d) . In this new equilibrium, there are again two moisture content areas after drainage, and the poten-

tial is constant in the horizontal. Thus, the first unstable infiltration flow sets a two-zoned initial moisture content field for future infiltration cycles in which each zone is on a different scanning curve of the moisture characteristic and each has a different initial conductivity.

In a subsequent infiltration event, because we start from equilibrium, the potential in the bottom layer at the textural interface is initially uniform in the horizontal, and thus the total potential gradient driving flow into the bottom layer does not vary in the horizontal either. At the interface and below, the moisture content and thus the conductivity vary because the core areas and fringe areas are on different scanning curves. The flow into the original core areas is therefore higher than into the fringe areas as long as the potentials in both areas are not too different during rewetting. When core and fringe areas are eventually wetted to the same potential at equilibrium (in the horizontal), their moisture contents and conductivities are again significantly different, yielding two distinct zones of moisture content and the persistence of the original unstable flow field. Because the two zones are in equilibrium, fingers may persist for a very long time or even indefinitely. For very long times, however, geochemical processes most certainly play a role.

The value of the potential at equilibrium in the second infiltration cycle may be different from that in the first for such reasons as the increased importance of air entrapment in initially wet porous media. Earlier qualitative observations of a second infiltration event indicated an increased participation of the fringe areas. If the fringe areas are wetter, the core areas must be drier at the same flow rate through the entire system. It is not obvious from earlier direct observation whether core areas go through a drying process behind the finger tip in the second cycle. However, it is clear that, in either case, fingers persist because of hysteresis in the moisture characteristic relation.

EXPERIMENTAL METHOD

To verify this theory for finger persistence, the moisture content structure and evolution of the unstable flow field must be carefully observed. First, it is necessary to document conclusively that drying occurs behind the finger tip in the first infiltration cycle and that core and fringe areas develop and coexist in the first and

in subsequent infiltration cycles. Because the time for finger tip wetting and drying during the initial stage is on a scale of seconds, a much more rapid technique than standard gamma-ray attenuation is necessary for measuring moisture content. A point-measurement method also is undesirable because the path of a finger is never known beforehand. Thus, a method that yields rapid relative moisture content at many points simultaneously in an entire slab of a porous medium is developed and applied to verify the theory.

The moisture-content-visualization technique is based on the physical observation that light transmission through sands increases with an increase in moisture content. Hoa et al. (1977) and Hoa (1981) first took advantage of this observation and developed a moisture-sensing probe that could measure moisture content at a point in a thin slab of a porous medium. They used an incandescent light bulb as the light-emitting source on one side and a light-sensitive photoresistor as the sensor on the other. They were able to obtain a calibration curve for the probe and use it in a study of the effects of hysteresis on transient flows in saturated and unsaturated porous media. Without a calibration curve, the moisture content of each point in the chamber can be related to that at other points to obtain a "relative" moisture content. To test the theory, only relative moisture content data are required, because these data allow visualization of moisture content changes and thus visualization of the evolution of the moisture content field.

Hoa's method is expanded to visualize moisture content in an entire two-dimensional flow field by supplying one side of a thin slab of a porous medium with a diffuse light source composed of a bank of high-output fluorescent light bulbs run by high-frequency ballasts (40 000 Hz). In a dry porous medium, the porosity, and, in a wet porous medium, the moisture content are immediately visible to the eye from the other side. The brighter the location, the higher the porosity and moisture content are in that location. The technique thus allows the rapid assessment of the homogeneity in the porous slab before the onset of infiltration.

The porosity in the initially dry porous medium and the evolution of the moisture content field during the course of an experiment are recorded on videotape using a standard video-camera with a zoom telephoto lens. The time

resolution is 1/30 s, the time resolution of the video equipment. Once on videotape, the images may be analyzed using any of the video-digitizing computer hardware and software packages available on the market. Our equipment makes use of a Frame Grabber board made by Data Translations, Inc., which can be installed in an IBM AT. Images may be digitized at will, stored, and manipulated to obtain gradients of light intensity, averages, differences between images, and the extent of wetted areas. A background image of the chamber before the onset of infiltration is subtracted from the digitized image to yield an image that shows only the moisture content in the chamber. With the use of a high-resolution color monitor, the images are displayed and false-colored according to light intensity at each location in the image, thus allowing the rapid visualization of the relative moisture content, (i.e., that a point is wetter relative to another point).

An earlier experiment with a Plexiglas slab chamber (Glass et al. 1987) was duplicated using a glass-sided slab chamber with a cross-sectional area 50×1 cm. The chamber was filled using a randomizer extension with an 80-cm-high bottom layer composed of a 20/30 fraction (U.S. sieve series) of commercial silica sand. A 10-cm-high, fine-textured top layer composed of 140/200 fraction silica sand was added and separated from the bottom layer by a piece of tissue paper. The light intensity field was recorded throughout a sequence of two ponded infiltration cycles. The first ponded infiltration cycle was conducted in the initially dry sand column for 2 wk. After 24 h of drainage without infiltration, a second ponded infiltration cycle followed.

RESULTS

The evolution of the moisture content field throughout the infiltration experiment is shown in a series of color photographs, Figs. 3 to 17. The region displayed in the photographs is 45 cm wide and 85 cm long (9 cm top layer, 76 cm bottom layer), bordered by dark blue. In all the photographs, the top layer is shown as a dark rectangular region at the top, below which fingers form. The relationship between light intensity and color and thus moisture content and color in the bottom layer is shown at the side of each image. The color sequence spans the range from black ($\theta = 0$) through blue, green, yellow, and orange to red ($\theta = \theta_s$, denoted as 1 in the images).

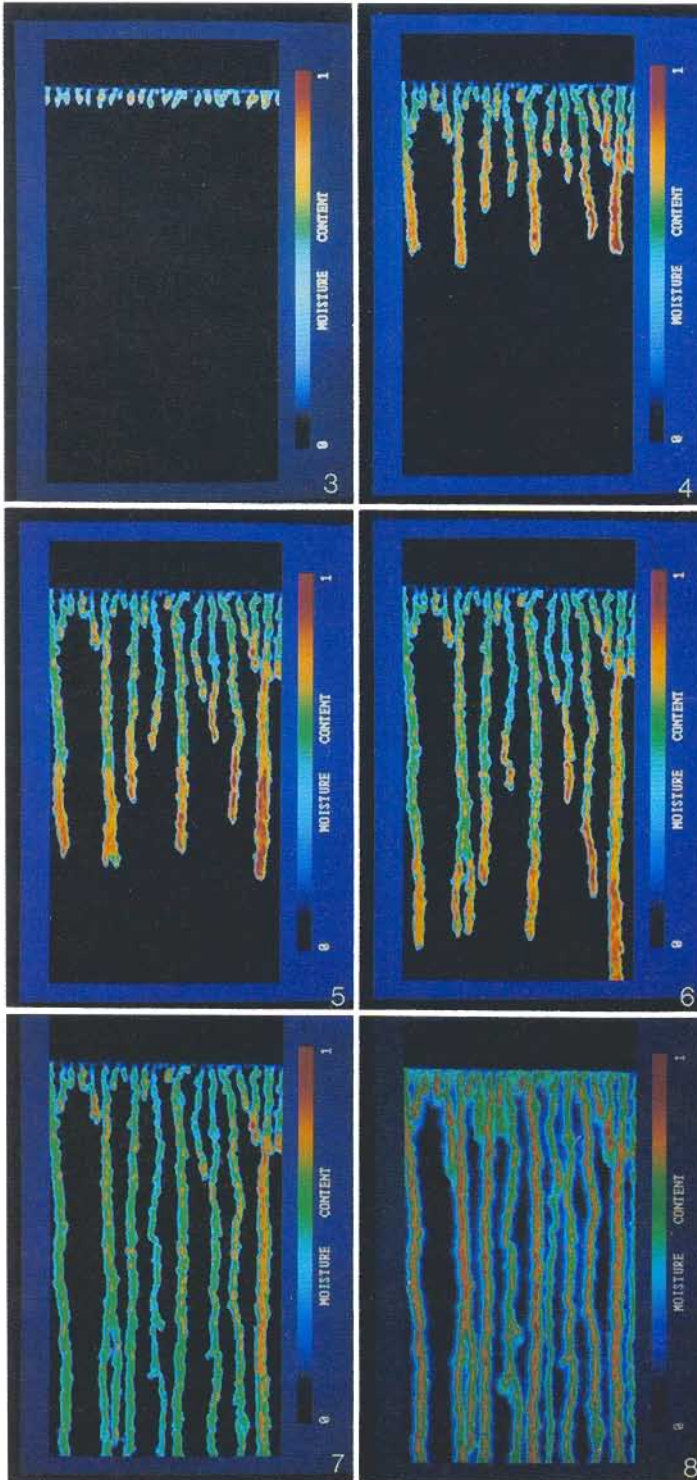


FIG. 3. Cycle 1, 2 min.

FIG. 4. Cycle 1, 4 min.

FIG. 5. Cycle 1, 5 min.

FIG. 6. Cycle 1, 6 min.

FIG. 7. Cycle 1, 15 min.

FIG. 8. Cycle 1, 2 d.

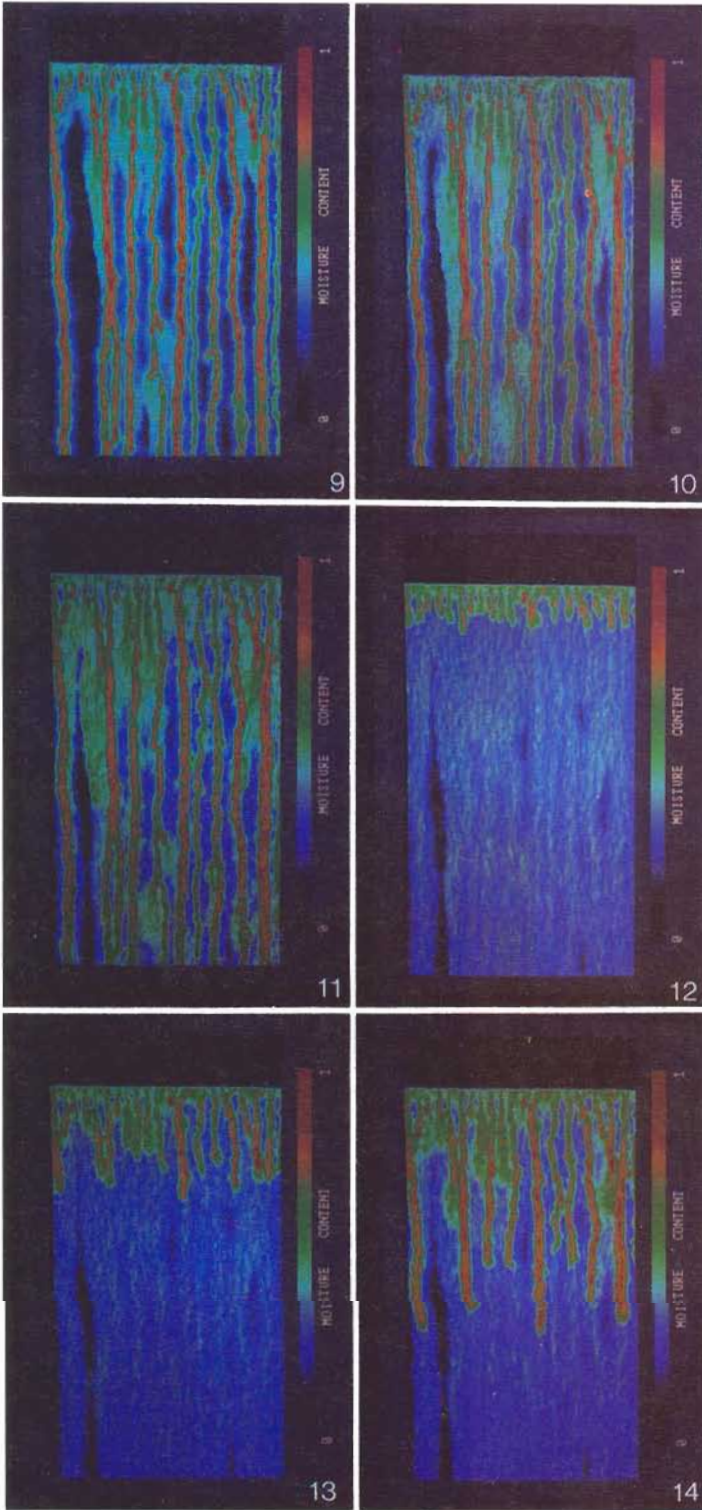


FIG. 9. Cycle 1, 7 d.

FIG. 10. Cycle 1, 14 d.

FIG. 11. Cycle 2, 1 min.

FIG. 12. Cycle 2, 2 min.

FIG. 13. Cycle 2, 4 min.

FIG. 14. Cycle 2, 6 min.

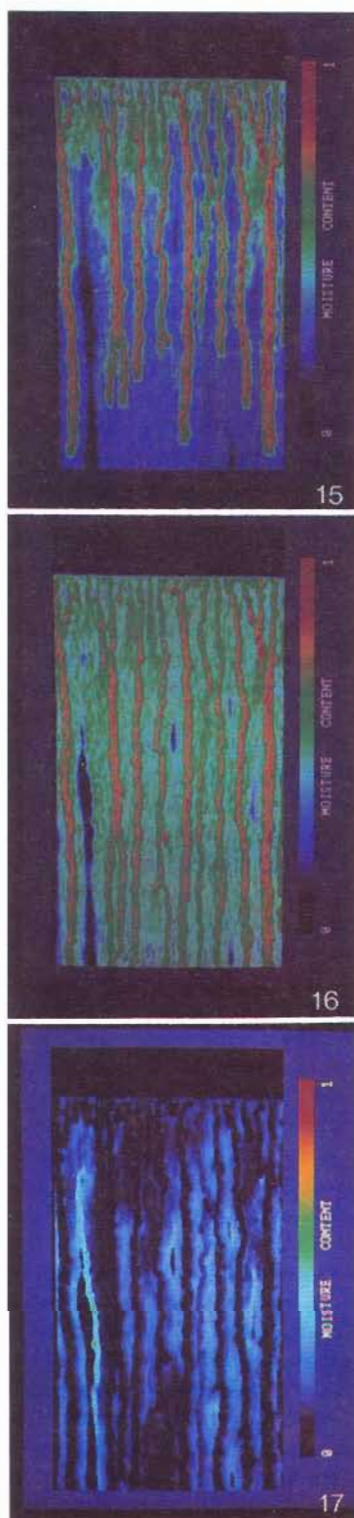


FIG. 15. Cycle 2, 15 min.
FIG. 16. Cycle 2, 8 h.

Cycle 1

Figure 3 shows the relative moisture content field 2 min after the onset of infiltration. The wetting front has just crossed the textural interface as a series of very uniformly spaced (approximately every 2 cm) "point sources." In each of these small fingers is a region of higher moisture content, which is visualized as a yellow to red area. Over the next minute, while the fingers are still near the textural interface, a large number of mergers takes place, reducing the number of fingers by over half (22 down to 9). The smaller number of stronger fingers is shown moving to the bottom of the chamber in Figs. 4, 5, and 6, at 4, 5, and 6 min, respectively. In this sequence, the finger tips are clearly shown to have a higher moisture content than the finger cores behind the tip, and the drying process is shown in every finger.

Figure 7 shows the moisture content field after 15 min of infiltration. All the fingers have reached the bottom of the chamber (off the photo) and are conducting water at a steady rate. Between 15 min and 4 h, the moisture content field changes very little. Subtraction of the two images shows a slight increase in moisture content around the edges of the fingers and a large increase in moisture content beneath several merger points where the tip of a slower finger had merged into another faster finger during the initial period (such as the initial finger to the left of the second main finger on the left). The slow development of the fringe area is shown in the sequence of photographs taken at 2, 7, and 14 d (Figs. 8, 9, and 10, respectively). A fairly uniform blue region about 2 to 3 cm wide has appeared around each of the finger core areas. In addition, two narrow fingers have appeared that were not part of the initial finger group that grew within the first 15 min. Each of these "dendrites" grew from a merger point. Areas below other merger points, although they have not formed separate fingers, have developed wetter regions and have enhanced fringe area growth. Even after 2 wk of steady infiltration, several small dry zones are visible between fingers, emphasizing the very long time scale of the horizontal wetting process.

FIG. 17. Subtraction of Cycle 1, 14-d image from Cycle 2, 8-h image.

Cycle 2

After a 24-h period of drainage with no inflow, the image of the initial moisture content field for the second cycle showed that variation in the initial moisture content was very small and that the locations of the original core areas were slightly wetter than in the surrounding fringe areas. Figures 11, 12, 13, and 14 show the reappearance of the original fingers as the second infiltration cycle proceeds. The velocity of all the fingers is almost the same; the fastest fingers in Cycle 1 slow down, and the slower fingers become faster. The increased fringe area contribution to flow is readily seen as the bottom layer wets and in Fig. 15, which was taken after 15 min of steady infiltration. This increased contribution causes a rapid transformation to the steady-state flow field shown in Fig. 16, which was taken after 8 h of steady infiltration. The correspondence of the 8-h field with that after 2 wk of steady infiltration in the first cycle is striking. Figure 17 is a subtraction of the Cycle 1, 14-d image (Fig. 10) from the Cycle 2, 8-h image (Fig. 16). In a subtraction, a negative result is set at zero so that if a region being subtracted is lighter than the region being subtracted from, the result will be zero (black). The subtraction of the images shown in the two figures indicates that the core areas of the image in the second cycle are dryer (black) and the fringe areas are wetter (light blue), although the structure is identical. It is also apparent that no drying takes place in the second cycle after the fringe tips have passed, and the finger tips do not fully saturate as they had in the first infiltration cycle into initially dry sand.

DISCUSSION

The evolution of the moisture content field as visualized using the optical technique clearly verifies that drying occurs behind finger tips in initially dry porous media. It also further documents the general flow-field development described in previous work (Glass and Steenhuis 1984; Glass et al. 1987) and thus the behavior, which is explained by the current theory based on hysteresis. The fact that the matric potential in a finger first increases as the tip wets and then decreases to the value ψ_c is demonstrated by finger tip drying and constant tip velocity. The fact that slower fingers always merge into faster fingers when they intersect the side of a

faster finger and not vice versa also indicates a decrease in matric potential from the finger tip upward. Hysteresis effects are also present at each merger point. When the finger tips of two merging fingers are not in the same horizontal plane (e.g., a slower finger merging into a faster finger behind the faster finger's tip), then because of hysteresis, the tip of the slower finger stays wetter than the associated point in the core of the faster finger, that is, the faster finger is now wetting on a scanning curve, while the slower finger is drying on the main drying curve. This effect can be seen quite clearly in Figs. 3 through 10.

It is also apparent that in initially dry porous media the finger tips all wet up to approximately the same value—very near saturation, denoted by the red color in the photographs—regardless of the finger width and velocity. Glass et al. (1989b) showed that the average moisture content of a finger, as determined by the flow per unit time divided by the volume wetted per unit time, is a function of the flow through a finger. In light of the current results, the average moisture content determined in this way corresponds to the average moisture content of the finger core and not of the finger tip. Because the tips of all fingers are saturated, the scaling of finger width is independent of the finger core moisture content. Glass et al. (1989a) gave the ratio $S_F^2/[K_F(\theta_F - \theta_s)]$ as the scaling factor for finger width, where S and K are the sorptivity and conductivity of the bottom layer, respectively, and the subscript F denotes evaluation at the moisture content of the finger θ_F . This ratio can be shown to be a weak function of θ near θ_s and was therefore replaced by $S^2/[(\theta_s - \theta_s)K_s]$, assuming that the fingers are nearly saturated as indeed the finger tips are.

Glass et al. (1989b) found, in initially dry porous media, that the wider the finger, the faster it moves. In our photographs, it can also be seen that the wider and faster the finger, the higher the saturated zone extends behind the tip of the finger, and the wetter the finger core area is once drying has taken place. This is clearly shown by comparing the fastest finger (last finger on the right) with one of the slowest fingers (e.g., the fourth finger from the left). The length of the saturated area, L_s , at all the finger tips is greater than $\psi_{we} - \psi_{ce}$, the difference between air entry value and the water entry value (approximately 10 cm for this sand). Fingers in

initially dry porous media may be thought of as short, saturated, hanging water columns being fed from above under essentially unit gradient at the rate $K(\theta_c)$. Finger tip velocity approaches a maximum of K_s/θ_c for high-flow fingers, when θ_c approaches θ_s and the entire finger becomes saturated. Glass et al. (1989b) observed this behavior; however, their results show that the finger width becomes infinite as θ_c approaches θ_s , and thus a stable one-dimensional flow field is forced. At the other extreme, fingers will stop moving when L_s approaches $\psi_{wc} - \psi_{ac}$. At this point, capillarity exactly offsets gravity, and, even though the tip is saturated, the finger does not move.

With this model, a simple relationship may be written for L_s as follows. Within the saturated area, the flux through the finger, q_F , may be written as

$$q_F = K_s \left[1 - \frac{\psi_{wc} - \psi_{ac}}{L_s} \right] \quad (3)$$

because the change in matric potential from the top of the saturated tip to the bottom is given by $\psi_{wc} - \psi_{ac}$. Thus, writing Eq. (3) in terms of the dimensionless flux-conductivity ratio, R_F , defined by the ratio of q_F and K_s yields

$$L_s = \frac{\psi_{wc} - \psi_{ac}}{1 - R_F} \quad (4)$$

Equation (4) has the behavior discussed above in the limit as R_F goes to 1 of becoming infinite and in the limit as R_F goes to 0 of approaching $\psi_{wc} - \psi_{ac}$.

The core/fringe area structural correspondence between the first and the second infiltration cycles is quite dramatic. The only time new fingers have been observed to form in the second cycle, and only occasionally, is when a region of the chamber is still dry at the onset of the cycle. Such was the case in the current experiment; however, no additional fingers formed.

The fact that finger tips are not saturated and that the area behind the tip does not dry suggests that the fingering mechanism in the two cycles is different. In the case of the first infiltration cycle in a uniform initial moisture content field in which θ_i is very low, the matric potential increases to near ψ_{wc} and then decreases to ψ_{ac} and below as a finger tip passes. In Cycle 2, the matric potential increases only as a tip moves by a fixed point. To more fully understand the

effects of initial moisture content and hysteresis on wetting front instability and, more generally, on the infiltration process itself, further experiments are being conducted with the use of the optical method.

CONCLUSIONS

We have demonstrated through the use of a new experimental technique that wetting front instability in initially dry porous media is dominated by hysteresis in the moisture characteristic relation. The formation of fingers with saturated tips that dry a distance behind the tip sets up a two-zone structure in the homogeneous coarse bottom layer that, as a result of hysteresis, persists for long and perhaps indefinite periods of steady infiltration and over subsequent infiltration events. More generally, the results of these experiments emphasize the importance of hysteresis in sandy soils, which, when combined with both temporal and spatial variation of flow caused either by instability or by intermittent water supply, can lead to the formation of persisting conduits of flow and extreme variability in solute transport.

ACKNOWLEDGMENTS

This research was supported in part by Environmental Protection Agency Grant R-812919-01-1: "Wetting Front Instability in Layered Soils and its Inclusion in Monitoring and Modeling Techniques." We wish to thank J. Throop for his help in developing the moisture visualization technique and G. H. Oosting and J. Nagy for their help in constructing the experimental apparatus.

REFERENCES

- Chouke, R. L., P. Van Meurs, and C. van der Poel. 1959. The instability of slow immiscible, viscous liquid-liquid displacements in porous media. *Trans. Am. Inst. Min. Eng.* 216:T.P.8073.
- Diment, G. A., and K. K. Watson. 1983. Stability analysis of water movement in unsaturated porous materials: 2. Numerical studies. *Water Resour. Res.* 19:1002-1010.
- Diment, G. A., and K. K. Watson. 1985. Stability analysis of water movement in unsaturated porous materials: 3. Experimental studies. *Water Resour. Res.* 21:979-984.
- Diment, G. A., K. K. Watson, and P. J. Blennerhassett. 1982. Stability analysis of water movement in unsaturated porous materials: 1. Theoretical considerations. *Water Resour. Res.* 18:1248-1254.
- Glass, R. J., J.-Y. Parlange, and T. S. Steenhuis. 1987.

- Water infiltration in layered soils where a fine textured layer overlays a coarse sand. Proceedings of the International Conference for Infiltration Development and Application, Hawaii, 5-9 Jan. 1987, pp. 66-81.
- Glass, R. J., J.-Y. Parlange, and T. S. Steenhuis. 1989a. Wetting front instability: 1. Theoretical discussion and dimensional analysis. *Water Resour. Res.* 25(6):1187-1194.
- Glass, R. J., and T. S. Steenhuis. 1984. Factors influencing infiltration flow instability and movement of toxics in layered sandy soils. ASAE technical paper 84-2508. ASAE St. Joseph, Mich.
- Glass, R. J., T. S. Steenhuis, and J.-Y. Parlange. 1988. Wetting front instability as a rapid and far-reaching hydrologic process in the vadose zone. *J. Contam. Hydrol.* 3:207-226.
- Glass, R. J., T. S. Steenhuis, and J.-Y. Parlange. 1989b. Wetting front instability: 2. Experimental determination of relationships between system parameters and two-dimensional unstable flow field behavior in initially dry porous media. *Water Resour. Res.* 25(6):1195-1207.
- Hill, S. 1952. Channeling in packed columns. *Chem. Eng. Sci.* 1:247-53.
- Hill, D. E., and J.-Y. Parlange. 1972. Wetting front instability in layered soils. *Soil Sci. Soc. Am. Proc.* 36:697-702.
- Hillel, D., and R. S. Baker. 1988. A descriptive theory of fingering during infiltration into layered soils. *Soil Sci.* 146:51-56.
- Hoa, N. T. 1981. A new method allowing the measurement of rapid variations on the water content in sandy porous media. *Water Resour. Res.* 17(1): 41-48.
- Hoa, N. T., R. Gaudu, and C. Thirriot. 1977. Influence of the hysteresis effect on transient flows in saturated-unsaturated porous media. *Water Resour. Res.* 13(6):992-996.
- Homsy, G. M. 1987. Viscous fingering in porous media. *Annu. Rev. Fluid Mech.* 19:271-311.
- Miller, D. E., and W. H. Gardner. 1962. Water infiltration into stratified soil. *Soil Sci. Soc. Am. Proc.* 26:115-119.
- Parlange, J.-Y., and D. E. Hill. 1976. Theoretical analysis of wetting front instability in soils. *Soil Sci.* 122:236-239.
- Peck, A. J. 1965. Moisture profile development and air compression during water uptake by bounded porous bodies: 3. Vertical columns. *Soil Sci.* 100:44-51.
- Philip, J. R. 1975a. Stability analysis of infiltration. *Soil Sci. Soc. Am. Proc.* 39:1042-1049.
- Philip, J. R. 1975b. The growth of disturbances in unstable infiltration flows. *Soil Sci. Soc. Am. Proc.* 39:1049-1053.
- Raats, P. A. C. 1973. Unstable wetting fronts in uniform and nonuniform soils. *Soil Sci. Soc. Am. Proc.* 37:681-685.
- Saffman, P. G., and G. Taylor. 1958. The penetration of a fluid into a porous medium or Hele-Shaw cell containing a more viscous liquid. *Proc. R. Soc. London.* A245:312-331.
- Smith, W. O. 1967. Infiltration in sand and its relation to ground water recharge. *Water Resour. Res.* 3:539-555.
- Starr, J. L., H. C. DeRoo, C. R. Frink, and J.-Y. Parlange. 1978. Leaching characteristics of a layered field soil. *Soil Sci. Soc. Am. J.* 42:376-391.
- Starr, J. L., J.-Y. Parlange, and C. R. Frink. 1986. Water and chloride movement through a layered field soil. *Soil Sci. Soc. Am. J.* 50:1384-1390.
- Tabuchi, T. 1961. Infiltration and ensuing percolation in columns of layered glass particles packed in laboratory. *Nogyo doboku kenkyn, Bessatsu* (Trans. Agric. Eng. Soc., Japan) 1:13-19.
- Tamai, N., T. Asaeda, and C. G. Jeevaraj. 1987. Fingering in two-dimensional, homogeneous, unsaturated porous media. *Soil Sci.* 144:107-112.
- White, I., P. M. Colombero, and J. R. Philip. 1976. Experimental study of wetting front instability induced by sudden change of pressure gradient. *Soil Sci. Soc. Am. J.* 40:824-829.
- White, I., P. M. Colombero, and J. R. Philip. 1977. Experimental studies of wetting front instability induced by gradual changes of pressure gradient and heterogeneous porous media. *Soil Sci. Soc. Am. J.* 41:483-489.